Directed Evolution

DOI: 10.1002/anie.200702616

Engineered Alkane-Hydroxylating Cytochrome $P450_{BM3}$ Exhibiting Nativelike Catalytic Properties**

*Rudi Fasan, Mike M. Chen, Nathan C. Crook, and Frances H. Arnold**

Cytochrome P450 enzymes (P450s) are exceptional oxygenating catalysts[1] with enormous potential in drug discovery, chemical synthesis, bioremediation, and biotechnology.[2,3] Compared to their natural counterparts, however, engineered P450s often exhibit poor catalytic and cofactor coupling efficiencies.[3] Obtaining native-like catalytic proficiencies is a mandatory first step towards utilizing the power of these versatile oxygenases in chemical synthesis.

Cytochrome $P450_{BM3}$ (119 kDa, *B. megaterium*) catalyzes the subterminal hydroxylation of long-chain (C_{12}–C_{20}) fatty acids.[4] Its high activity and catalytic self-sufficiency (heme and diflavin reductase domains are fused in a single polypeptide chain)[2,4,5] make $P450_{BM3}$ an excellent platform for biocatalysis. However, despite numerous reports of the heme domain being engineered to accept nonnative substrates, including short-chain fatty acids, aromatic compounds, alkanes, and alkenes,[6–8] reports of preparative-scale applications of $P450_{BM3}$ remain scarce.[9]

$P450_{BM3}$ function is finely regulated through conformational rearrangements in the heme and reductase domains and possibly also through hinged domain motions.[4,10] Hydroxylation of fatty acids occurs almost fully coupled to cofactor (NADPH) utilization (93–96% depending on the substrate).[11] In the presence of nonnative substrates or when amino acid substitutions are introduced, the mechanisms controlling efficient catalysis in P450s are disrupted,[12] leading to the formation of reactive oxygen species and rapid enzyme inactivation.[4] High coupling efficiencies on substrates whose physicochemical properties are substantially different from the native substrates have not been achieved, and coupling efficiencies ranging from less than 1% to 30–40% are typical.[7,8] Strategies for addressing this "coupling problem" are needed in order to take engineered P450s to larger-scale applications.

Selective hydroxylation of short alkanes is a long-standing problem, for which no practical catalysts are available.[13] In an effort to produce $P450_{BM3}$-based biocatalysts for selective hydroxylation of small alkanes, we previously engineered this enzyme to accept propane and ethane (35E11 variant).[14] Despite greater than 5000 total turnover (TTN) supported in vitro, the utility of this catalyst remained limited because of its poor in vivo performance (see below), which was mostly due to the low efficiencies for coupling the product formation to cofactor consumption (17.4% for propane and 0.01% for ethane oxidation).

Our goal was to engineer a $P450_{BM3}$ variant with native-like activity and coupling efficiency towards a structurally challenging, nonnative substrate (propane) and evaluate the impact of these features on performance in preparative-scale biotransformations. To this end, we used a domain-based protein-engineering strategy, in which the heme, flavin mononucleotide (FMN), and flavin adenine dinucleotide (FAD) domains of the 35E11 variant were evolved separately in the context of the holoenzyme, and beneficial mutations were recombined in a final step (Figure 1). Previous work suggested that mutations in the reductase and linker regions can affect catalytic properties.[14,15] However, no systematic engineering efforts had been undertaken to engineer the complete 1048 amino acid holoenzyme.

Holoenzyme libraries outlined in Figure 1 were created using random, saturation, and site-directed mutagenesis and

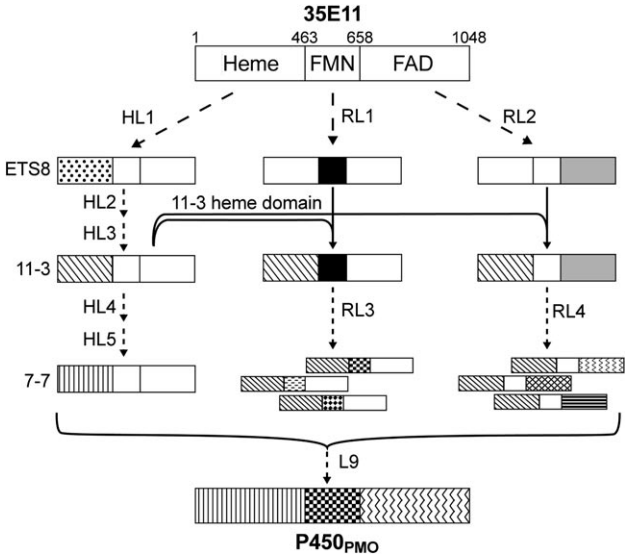

Figure 1. Outline of the domain engineering strategy used to improve cytochrome $P450_{BM3}$ heme and reductase domains. HL = heme domain libraries, RL = reductase domain libraries.

[*] Dr. R. Fasan, M. M. Chen, N. C. Crook, Prof. Dr. F. H. Arnold
Department of Chemistry and Chemical Engineering
California Institute of Technology
1200 California Blvd. MC 210-41, Pasadena, CA 91125 (USA)
Fax: (+1) 626-568-8743
E-mail: frances@cheme.caltech.edu

[**] This work was supported by a Swiss National Science Foundation fellowship to R.F., a U.S. NSF Fellowship to M.M.C. and by the U.S. Army Research Office, ARO Contract DAAD19-03-D-0004. We thank Dr. Christopher Snow for providing the homology model of $P450_{BM3}$ reductase and Dr. Matthew W. Peters, Dr. Peter Meihnold, and Dr. Marco Landwehr for helpful discussions regarding the biotransformations and for providing access to DasGip fermenter.

Supporting information for this article is available on the WWW under http://www.angewandte.org or from the author.

screened for activity on a propane surrogate, dimethyl ether.[8] Positives were confirmed in a re-screen, purified, and challenged with propane in sealed vials in the presence of a cofactor regeneration system. As a cumulative measure of both catalytic and coupling efficiency, improvement in total turnover (moles of propanol produced per mole of enzyme) was used as the sole selection criterion.

Measurement of the half-denaturation temperature of 35E11 heme domain demonstrated a considerable reduction in its stability as a consequence of the 15 accumulated mutations ($T_{50} = 43.4\,^{\circ}C$ vs. $55.0\,^{\circ}C$ for wild type). We therefore subjected 35E11 to an initial thermostabilization step (HL1), in which stabilizing mutations from a thermostable $P450_{BM3}$ peroxygenase[16] were tested singly and in combination in the 35E11 background (see the Supporting Information). Variant ETS8 ($\Delta T_{50} = +5.1\,^{\circ}C$, $\Delta TTN_{propane} = -1250$) showed the best combination of increased stability with little decrease in TTN and was selected for further directed evolution. Using ETS8 as parent, heme-domain random mutagenesis libraries were generated by error-prone PCR (HL2). Variant 19A12, with about twofold increase in TTN (Table 1), was then used to create a pool of active-site libraries (HL3) in which 17 positions along the substrate channel (Figure 2a) and near the active site (Figure 2b) were subjected individually to saturation mutagenesis. Further improvements in propane-hydroxylating activity were achieved in multiple variants, including 11-3. Recombination of the beneficial mutations from the active-site libraries (HL4) led to variant 1-3. Further fine-tuning of the active site was pursued with a series of recombination/site-saturation libraries (HL5, see Supporting Information). From these libraries, 7-7 emerged as the most active variant, supporting 20500 turnovers with propane.

Meanwhile, two libraries were constructed in which random mutations were targeted to the FMN- and FAD-binding domains of 35E11 (RL1 and RL2, respectively). Screening of more than 5000 members from each library led to the identification of eight beneficial mutations (G443D, V445M, T480M, T515M, P654Q, T664M, D698G, and E1037G).[17] These positions were further optimized by saturation mutagenesis in a holoenzyme construct having the 11-3 heme domain (RL3, RL4). Swapping the heme domains this way serves to remove mutations whose beneficial effect is solely dependent on the presence of the 35E11 heme domain. Improved 11-3-derived variants were found to contain G443A, V445R, P654K, T664G, D698G, and E1037G mutations and showed TTN between 16000 and 20000. In the final step, a library containing the beneficial reductase domain mutations was fused to the heme domain of variant 7-7 (L9). The most active variant isolated from this library, $P450_{PMO}R2$, supported more than 45000 turnovers and produced 2- and 1-propanol in a 9:1 ratio. As we expected, the increase in productivity strongly correlates with the increase in coupling efficiency, which in the best variant ($P450_{PMO}R2$, 98.2%) reaches levels comparable to those measured for wild-type in the hydroxylation of myristate (88%), palmitate (93%), or laurate (96%).[11]

The sequence of mutational events leading to $P450_{PMO}$ generation reveals a continuous rearrangement of substrate-channel and active-site residues (Table 1), presumably in search of an optimal configuration for accommodating propane. Additional beneficial mutations in the hydroxylase domain include L188P and G443A. Leucine 188 is located along helix F, which together with helix G forms a lid covering

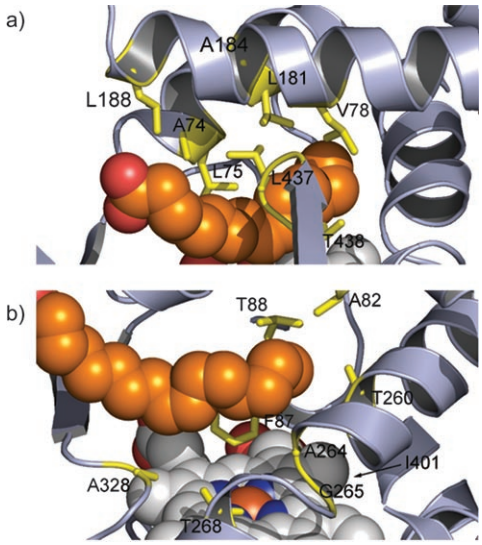

Figure 2. a) Substrate channel and b) active-site residues targeted for saturation mutagenesis mapped on the palmitate-bound structure of $P450_{BM3}$ heme domain (PDB 1FAG[26]). Heme (white) and fatty acid (orange) are shown in space-filling mode.

Table 1: In vitro propane oxidation activities of most representative $P450_{BM3}$ variants.[a]

Variant	Library	Mutations versus 35E11[b]		Rate[c] [equiv min^{-1}]	Coupling[d] [%]	Total turnovers
		heme domain	reductase domain			
35E11	–	–	–	210	17.4	5650
19A12	HL2	L52I, L188P, I366V	–	420	44.2	10550
11-3	HL3	L52I, A74S, L188P, I366V	–	390	55.3	13200
698E5	RL3	L52I, A74S, L188P, I366V	D698G	295	65.3	17300
1-3	HL4	L52I, A74S, V184A, L188P, I366V	–	320	72.1	19200
7-7	HL5	L52I, A74E, S82G, A184V, L188P, I366V	–	150	90.9	20500
$P450_{PMO}R1$	L9	L52I, A74E, S82G, A184V, L188P, I366V, G443A	P654K, E1037G	455	94.4	35600
$P450_{PMO}R2$	L9	L52I, A74E, S82G, A184V, L188P, I366V, G443A	D698G	370	98.2	45800

[a] Mean values from at least three replicates ±10% error. [b] Mutations in 35E11 are R47C, V78F, A82S, K94I, P142S, T175I, A184V, F205C, S226R, H236Q, E252G, R255S, A290V, A328F, L353V, E464G, I710T. [c] Over the first 20 s. [d] Ratio between propanol formation rate and NADPH oxidation rate in propane-saturated buffer.

the active site.[18] Glycine 443 lies on a loop at the C-terminal end of hairpin β4, which inserts into the active site.[18]

Interestingly, the activity-enhancing substitutions in the reductase domain are clustered in the same region in the FAD domain (T664G, D698G, E1037G) and nearby linker to the FMN domain (P654K; see map in the Supporting Information). Perturbation of electrostatic charge distribution appears to be a prevailing trend, suggesting a more important role of these forces in $P450_{BM3}$ function than previously proposed.[19] A smaller contribution was obtained by mutating the FMN domain. This effect may reflect its higher sensitivity to mutagenesis, as judged by the significantly lower fraction of functional variants in the FMN libraries compared to the FAD libraries (data not shown). Chemical and thermal denaturation studies have shown that, among the three cofactors, FMN is most weakly bound to the enzyme.[20]

A common strategy to reduce the prohibitive costs of NADPH-driven biotransformations is the use of cofactor regeneration systems.[9c,21] For bulk chemical transformations such as alkane hydroxylation, these in vitro approaches are not viable.[22] The propane-hydroxylating P450 variants were therefore evaluated in whole-cell biotransformations using resting *E. coli* cells (Figure 3).

The expression levels of these variants in minimal medium (initially less than 0.5% of total cell mass) were first optimized to achieve 6–11% of total cell mass as soluble P450 enzyme. Experiments were carried out in a 100-mL fermenter using cell suspensions in nitrogen-free minimal medium (supplemented with glucose) and a propane/air mixture as substrate and oxidant feed. Under these conditions, cell densities less than 1 g cdw L^{-1} (typically 0.5–0.9 g cdw L^{-1}; cdw = cell dry weight) were used to avoid oxygen-transfer limitations. Activities of 80–120 U g^{-1} cdw (where 1 U = 1 μmol propanol min^{-1}) were measured for $P450_{PMO}R1$ and $P450_{PMO}R2$ in various *E. coli* strains (Figure 3a, Table 2). The experiment was repeated in a larger fermenter (0.3 L, pH and dissolved oxygen control). A suspension of P450-expressing DH5α cells was fed with a 1:1 mixture of pure oxygen and propane, and propanol formation was monitored for up to 9 h (Figure 3b). Under these conditions, very high activities (up to 180 U g^{-1} cdw) were obtained. In comparison, maximal activities of 30 U g^{-1} cdw on *n*-nonene were reported for the natural AlkB alkane hydroxylase system in both homologous (*P. oleovorans*) and heterologous strains (*E. coli*).[23a]

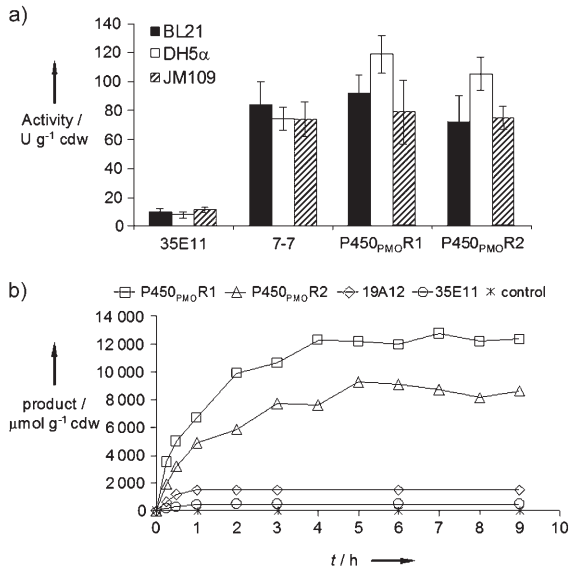

Figure 3. Whole-cell biotransformation of propane. a) Initial activities of selected $P450_{BM3}$ variants in different *E. coli* strains using air/propane (1:1) feed (pH 7.2, 25 °C). b) Time course of propane biotransformation using recombinant DH5α cells using oxygen/propane (1:1) feed (pH 7.2, 25 °C). Product amount is given per gram cell dry weight to facilitate comparison among variants. Control: no propane in the gas feed.

Table 2: In vivo propane oxidation activities of $P450_{BM3}$ variants.[a]

Variant	Oxidant (propane/oxidant ratio)	Activity[b] [U g^{-1} cdw] 0.5 h	3 h	Productivity[b,c] [mmol propanol g^{-1} P450 h^{-1}]
35E11	air (1:1)	9	2	12
19A12	air (1:1)	41	9	44
7-7	air (1:1)	74	n.d.	88
$P450_{PMO}R1$	air (1:1)	118	73	119
$P450_{PMO}R2$	air (1:1)	104	68	106
$P450_{PMO}R1$	O_2 (1:1)	176	63	96
$P450_{PMO}R2$	O_2 (1:1)	119	39	94

[a] Mean values from two biological replicates ±15% error. n.d. = not determined. [b] At cell density = 0.5–0.9 g cdw L^{-1}. [c] Calculated from the first hour of biotransformation.

At moderately higher cell densities (ca. 4 g cdw L^{-1}), propanol accumulated to a concentration of more than 15 mM over 4 h (Figure 4, upper panel). The improved coupling efficiencies result in considerably extended periods of whole-cell activity (6 vs. 0.5 h, Figures 3b and 4). To investigate the possible causes of the decrease in productivity over time, we monitored the biocatalyst concentration over the course of the biotransformation (Figure 4, lower panel). At the end of the experiment, approximately 52% of the

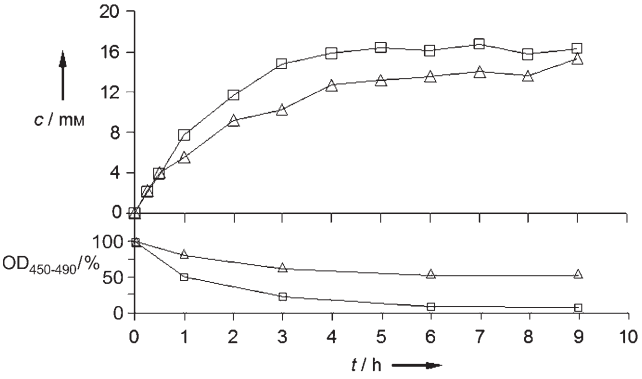

Figure 4. Concentration of propanol during biotransformation of propane with DH5α cells expressing $P450_{PMO}R1$ (□) and $P450_{PMO}R2$ (△) at medium cell density (4 g cdw L^{-1}). In the lower panel, relative P450 concentration as determined from CO-binding difference spectra on cell lysate; OD = optical density.

initial $P450_{PMO}R2$ was still correctly folded in the cells. Control experiments using $P450_{PMO}R2$-expressing cells and propanol concentrations up to 30 mM showed no product inhibition nor overoxidation to acetone, suggesting that host-related rather than biocatalyst-dependent factors are limiting. Indeed, 40–60% of the initially measured activity could be restored by resuspending cells from the plateau phase (i.e. after 4–6 h reaction) in fresh medium. In addition, the rate of biocatalyst inactivation could be reduced by varying the relative concentration of oxygen in the gas feed, with more extended whole-cell activity periods obtained at a propane/oxygen ratio of 4:1 compared to 1:1 (Table 2). Optimization of this parameter as well as the availability of more robust host strains[22] is expected to further enhance the whole-cell productivity of this engineered $P450_{BM3}$.

Overall, a domain-based directed evolution strategy has enabled us to engineer a finely-tuned, multicofactor, multidomain enzyme to exhibit nativelike catalytic properties on a substrate significantly different from the native substrate. With this approach, we could use relatively small and targeted libraries to identify beneficial mutations throughout the enzyme, which were recombined to yield the most efficient engineered P450 reported to date. This strategy should prove useful for engineering other enzymes with multiple, interacting functional domains. With high activity and coupling efficiency for propane oxidation, $P450_{PMO}$s could be used in whole-cell biohydroxylation of propane at room temperature and pressure with air as oxidant. Total activities and product formation rates exceeding those obtained with naturally occurring alkane monooxygenases on their native substrates[23,24] were achieved in this first report of whole-cell bioconversion of propane to propanol in *E. coli*.[25] These results open the door to considering P450-based oxidations of short-chain alkanes, with promise for green conversion of gaseous hydrocarbons into liquid fuels and chemicals.

Received: June 15, 2007
Published online: September 20, 2007

Keywords: alkane oxidation · biotransformations · cytochrome P450 · directed evolution · protein engineering

[1] a) M. Sono, M. P. Roach, E. D. Coulter, J. H. Dawson, *Chem. Rev.* **1996**, *96*, 2841–2888; b) I. G. Denisov, T. M. Makris, S. G. Sligar, I. Schlichting, *Chem. Rev.* **2005**, *105*, 2253–2277.

[2] V. B. Urlacher, S. Eiben, *Trends Biotechnol.* **2006**, *24*, 324–330.

[3] R. Bernhardt, *J. Biotechnol.* **2006**, *124*, 128–145.

[4] A. W. Munro, D. G. Leys, K. J. McLean, K. R. Marshall, T. W. Ost, S. Daff, C. S. Miles, S. K. Chapman, D. A. Lysek, C. C. Moser, C. C. Page, P. L. Dutton, *Trends Biochem. Sci.* **2002**, *27*, 250–257.

[5] A. J. Warman, O. Roitel, R. Neeli, H. M. Girvan, H. E. Seward, S. A. Murray, K. J. McLean, M. G. Joyce, H. Toogood, R. A. Holt, D. Leys, N. S. Scrutton, A. W. Munro, *Biochem. Soc. Trans.* **2005**, *33*, 747–753.

[6] a) T. W. Ost, C. S. Miles, J. Murdoch, Y. Cheung, G. A. Reid, S. K. Chapman, A. W. Munro, *FEBS Lett.* **2000**, *486*, 173–177; b) W. T. Sulistyaningdyah, J. Ogawa, Q. S. Li, C. Maeda, Y. Yano, R. D. Schmid, S. Shimizu, *Appl. Microbiol. Biotechnol.* **2005**, *67*, 556–562; c) D. Appel, S. Lutz-Wahl, P. Fischer, U. Schwaneberg, R. D. Schmid, *J. Biotechnol.* **2001**, *88*, 167–171; d) A. Glieder, E. T. Farinas, F. H. Arnold, *Nat. Biotechnol.* **2002**, *20*, 1135–1139; e) Q. S. Li, J. Ogawa, R. D. Schmid, S. Shimizu, *FEBS Lett.* **2001**, *508*, 249–252; f) T. Kubo, M. W. Peters, P. Meinhold, F. H. Arnold, *Chem. Eur. J.* **2006**, *12*, 1216–1220.

[7] a) Q. Li, J. Ogawa, R. D. Schmid, S. Shimizu, *Appl. Environ. Microbiol.* **2001**, *67*, 5735–5739; b) A. B. Carmichael, L. L. Wong, *Eur. J. Biochem.* **2001**, *268*, 3117–3125.

[8] M. W. Peters, P. Meinhold, A. Glieder, F. H. Arnold, *J. Am. Chem. Soc.* **2003**, *125*, 13442–13450.

[9] a) S. Schneider, M. G. Wubbolts, G. Oesterhelt, D. Sanglard, B. Witholt, *Biotechnol. Bioeng.* **1999**, *64*, 333–341; b) R. J. Sowden, S. Yasmin, N. H. Rees, S. G. Bell, L. L. Wong, *Org. Biomol. Chem.* **2005**, *3*, 57–64; c) J. R. Falck, K. Y. Reddy, D. C. Haines, K. M. Reddy, U. M. Krishna, S. Graham, B. Murry, J. A. Peterson, *Tetrahedron Lett.* **2001**, *42*, 4131–4133; d) S. C. Maurer, K. Kuhnel, L. A. Kaysser, S. Eiben, R. D. Schmid, V. B. Urlacher, *Adv. Synth. Catal.* **2005**, *347*, 1090–1098. Among these, only two examples involve a nonnative substrate, with the highest TTN (12850) achieved by Maurer et al. on cyclohexane over a 100-h period using an isolated $P450_{BM3}$ variant, a cofactor regeneration system, and a cyclohexane/buffer biphasic system.

[10] a) D. C. Haines, D. R. Tomchick, M. Machius, J. A. Peterson, *Biochemistry* **2001**, *40*, 13456–13465; b) M. B. Murataliev, R. Feyereisen, *Biochemistry* **1996**, *35*, 15029–15037.

[11] a) M. A. Noble, C. S. Miles, S. K. Chapman, D. A. Lysek, A. C. Mackay, G. A. Reid, R. P. Hanzlik, A. W. Munro, *Biochem. J.* **1999**, *339*, 371–379; b) M. J. Cryle, R. D. Espinoza, S. J. Smith, N. J. Matovic, J. J. De Voss, *Chem. Commun.* **2006**, 2353–2355.

[12] a) P. J. Loida, S. G. Sligar, *Biochemistry* **1993**, *32*, 11530–11538; b) S. Kadkhodayan, E. D. Coulter, D. M. Maryniak, T. A. Bryson, J. H. Dawson, *J. Biol. Chem.* **1995**, *270*, 28042–28048.

[13] a) J. A. Labinger, J. E. Bercaw, *Nature* **2002**, *417*, 507–514; b) G. B. Shul'pin, G. Suss-Fink, L. S. Shul'pina, *J. Mol. Catal. A* **2001**, *170*, 17–34; c) I. Yamanaka, S. Hasegawa, K. Otsuka, *Appl. Catal. A* **2002**, *226*, 305–315.

[14] P. Meinhold, M. W. Peters, M. M. Chen, K. Takahashi, F. H. Arnold, *ChemBiochem* **2005**, *6*, 1765–1768; Wong and coworkers have recently reported an engineered P450cam for in vitro hydroxylation of propane and ethane (F. Xu, S. G. Bell, J. Lednik, A. Insley, Z. Rao, L.-L. Wong , *Angew. Chem.* **2005**, *117*, 4097–4100; *Angew. Chem. Int. Ed.* **2005**, *44*, 4029–4032) using a reconstituted redox system containing $P450_{cam}$/putidaredoxin/putidaredoxin reductase in a 1:16:1 ratio.

[15] a) S. Govindaraj, T. L. Poulos, *Biochemistry* **1995**, *34*, 11221–11226; b) O. Roitel, N. S. Scrutton, A. W. Munro, *Biochemistry* **2003**, *42*, 10809–10821.

[16] O. Salazar, P. C. Cirino, F. H. Arnold, *ChemBiochem* **2003**, *4*, 891–893.

[17] Residues G443 and V445 are in the heme domain. The region targeted for construction of FMN libraries comprises 32 residues located at the C-terminus of $P450_{BM3}$ heme domain, which are not included in the heme domain libraries (see the Supporting Information).

[18] O. Pylypenko, I. Schlichting, *Annu. Rev. Biochem.* **2004**, *73*, 991–1018.

[19] D. R. Davydov, A. A. Kariakin, N. A. Petushkova, J. A. Peterson, *Biochemistry* **2000**, *39*, 6489–6497.

[20] A. W. Munro, J. G. Lindsay, J. R. Coggins, S. M. Kelly, N. C. Price, *Biochim. Biophys. Acta Protein Struct. Mol. Enzymol.* **1996**, *1296*, 127–137.

[21] a) U. Schwaneberg, C. Otey, P. C. Cirino, E. Farinas, F. H. Arnold, *J. Biomol. Screening* **2001**, *6*, 111–117; b) S. C. Maurer, H. Schulze, R. D. Schmid, V. B. Urlacher, *Adv. Synth. Catal.* **2003**, *345*, 802–810.

[22] W. A. Duetz, J. B. van Beilen, B. Witholt, *Curr. Opin. Biotechnol.* **2001**, *12*, 419–425.

[23] a) I. E. Staijen, J. B. Van Beilen, B. Witholt, *Eur. J. Biochem.* **2000**, *267*, 1957 – 1965; b) T. Fujii, T. Narikawa, K. Takeda, J. Kato, *Biosci. Biotechnol. Biochem.* **2004**, *68*, 2171 – 2177; c) M. Kubota, M. Nodate, M. Yasumoto-Hirose, T. Uchiyama, O. Kagami, Y. Shizuri, N. Misawa, *Biosci. Biotechnol. Biochem.* **2005**, *69*, 2421 – 2430.

[24] a) T. Furuto, M. Takeguchi, I. Okura, *J. Mol. Catal. A* **1999**, *144*, 257 – 261; b) S. G. Lee, J. H. Goo, H. G. Kim, J.-I. Oh, Y. M. Kim, S. W. Kim, *Biotechnol. Lett.* **2004**, *26*, 947 – 950.

[25] Previous whole-cell bioconversions of gaseous alkanes have relied on partial inhibition (i.e. blockage of methanol dehydrogenase activity) of methanotrophic bacteria carrying multicomponent nonheme methane monooxygenases.[24] Accumulations of 5–8 mM methanol over periods of 40 h were reported.

[26] H. Li, T. L. Poulos, *Nat. Struct. Biol.* **1997**, *4*, 140 – 146.

Angewandte Chemie
Eine Zeitschrift der Gesellschaft Deutscher Chemiker

Supporting Information

69451 Weinheim, Germany

Engineered alkane-hydroxylating cytochrome $P450_{BM3}$ exhibiting native-like catalytic properties

Rudi Fasan, Mike M. Chen, Nathan C. Crook, Frances H. Arnold*

Department of Chemistry and Chemical Engineering, California Institute of Technology, 91125 Pasadena (CA), U.S.A.

Experimental Section

Plasmids and oligonucleotides. Plasmid pCWori[1] was used as cloning vector. Oligonucleotides were purchased from Invitrogen (Carlsbad, CA). The sequence of the primers used in this study are reported below:

#	Primer name	Sequence
1	L52I_for	5'-CGC GCT ACA TAT CAA GTC AGC-3'
2	L52I_rev	5'-GCT GAC TTG ATA TGT AGC GCG-3'
3	M145A_for	5'-GTA TCG GAA GAC GCG ACA CGT TTA ACG-3'
4	M145A_rev	5'-GTA TCG GAA GAC GCG ACA CGT TTA ACG-3'
5	V340M_for	5'-GAA GAT ACG ATG CTT GGA GGA G-3'
6	V340M_rev	5'-CTC CTC CAA GCA TCG TAT CTT C-3'
7	I366V_for	5'-CGT GAT AAA ACA GTT TGG GGA GAC G-3'
8	I366V_rev	5'-CGT CTC CCC AAA CTG TTT TAT CAC G-3'
9	E442K_for	5'-CGT TAA AAC CTA AAG GCT TTG TGG-3'
10	E442K_rev	5'-CCA CAA AGC CTT TAG GTT TTA ACG-3'
11	L324I_for	5'-CGA AGC GCT GCG CAT CTG GCC AAC TT-3'
12	L324I_rev	5'-AAG TTG GCC AGA TGC GCA GCG CTT CG-3'
13	S106R_for	5'-CTTACTTCCAAGGTTCAGTCAGCAGG-3'
14	S106R_rev	5'-CCT GCT GAC TGA ACC TTG GAA GTA AG-3'
15	BamHI_fwd	5'-CAC AGG AAA CAG GAT CCA TCG ATG CTT AGG-3'
16	SacI_rev	5'-CTA GGT GAA GGA ATA CCG CCA AGC GGA-3'
17	L437NNK_for	5'-CGA TAT TAA AGA AAC TNN KAC GTT AAA ACC-3'
18	L437NNK_rev	5'-GGT TTT AAC GTM NNA GTT TCT TTA ATA TCG-3'
19	T438NNK_for	5'-CGA TAT TAA AGA AAC TTT ANN KTT AAA ACC-3'
20	T438NNK_rev	5'-GGT TTT AAM NNT AAA GTT TCT TTA ATA TCG-3'
21	EcoRI_Rev	5'-CCG GGC TCA GAT CTG CTC ATG TTT GAC AGC-3'
22	L181NNK_for	5'-GGT CCG TGC ANN KGA TGA AGT AAT G-3'
23	L181NNK_rev	5'-CAT TAC TTC ATC MNN TGC ACG GAC C-3'
24	A82NNK_for	5'-CGT GAT TTT NNK GGA GAC GGG TTA-3'
25	A82NNK_rev	5'-TAA CCC GTC TCC MNN AAA ATC ACG-3'
26	A74NNK_for	5'-AAC TTA AGT CAA NNK CTT AAA TTC-3'
27	A74NNK_rev	5'-GAA TTT AAG MNN TTG ACT TAA GTT-3'
28	L75NNK_for	5'-GTC AAG CGN NK AAA TTC TTT CGT G-3'

29	L75NNK_rev	5’-CAC GAA AGA ATT TMN NCG CTT GAC-3’
30	V78NNK_for	5’-GTC AAG CGC TTA AAT TCN NKC GTG ATT TT-3’
31	V78NNK_rev	5’-AAA ATC ACG MNN GAA TTT AAG CGC TTG AC-3’
32	A328NNK_for	5’-GGC CAA CTN NKC CTG CGT TTT CC-3’
33	A328NNK_rev	5’-GGA AAA CGC AGG MNN AGT TGG CC-3’
34	A184NNK_for	5’-GCA CTG GAT GAA NNK ATG AAC AAG-3’
35	A184NNK_rev	5’-CTT GTT CAT MNN TTC ATC CAG TGC-3’
36	L188NNK_for	5’-GAA CAA GNN KCA GCG AGC AAA TCC-3’
37	L188NNK_rev	5’-GGA TTT GCT CGC TGM NNC TTG TTC-3’
38	I401NNKfwd	5’-GCG TGC GTG TNN KGG TCA GCA G-3’
39	I401NNKrev	5’-CTG CTG ACC MNN ACA CGC ACG C-3’
40	T268NNKfwd	5’-GCG GGA CAC GAA NNK ACA AGT GGT C-3’
41	T268NNKrev	5’-GAC CAC TTG TMN NTT CGT GTC CCG C-3’
42	G265NNKfwd	5’-CAT TCT TAA TTG CGN NKC ACG AAA CAA CAA GTG-3’
43	G265NNKrev	5’-CAC TTG TTG TTT CGT GMN NCG CAA TTA AGA ATG-3’
44	A264NNKfwd	5’-CA TTC TTA ATT NNK GGA CAC GAA ACA ACA AGT G-3’
45	A264NNKrev	5’-CAC TTG TTG TTT CGT GTC CMN NAA TTA AGA ATG-3’
46	T260NNKfwd	5’-CAA ATT ATT NNK TTC TTA ATT GCG GGA C-3’
47	T260NNKrev	5’-GTC CCG CAA T TA AGA AMN NAA TAA TTT G-3’
48	L75NNKfwd	5’-GTC AAG CGN NKA AAT TTG TAC G-3’
49	L75NNKrev	5’-GTC CCG CAA TTA AGA AMN NAA TAA TTT G-3’
50	T88NNKfwd	5’-GAC GGG TTA TTT NNK AGC TGG ACG CAT G-3’
51	T88NNKrev	5’-GTC CCG CAA TTA AGA AMN NAA TAA TTT G-3’
52	F87NNKfwd	5’-GAC GGG TTA NNK ACA AGC TGG-3’
53	F87NNKrev	5’-CCA GCT TGT MNN TAA CCC GTC-3’
54	A82G_for	5’-CGT GAT TTT GGT GGA GAC GGG TTA-3’
55	A82G_rev	5’-TAA CCC GTC TCC ACC AAA ATC ACG-3’
56	FMN_for	5’-GCT GGT ACT TGG TAT GAT GCT-3’
57	FMN_rev	5’-CCA GAC GGA TTT GCT GTG AT-3’
58	FAD_for	5’-CGT GTA ACA GCA AGG TTC GG-3’
59	FAD_rev	5’-CTG CTC ATG TTT GAC AGC TTA TC-3’
60	G443NNK_for	5’-CGT TAA AAC CTG AAN NKT TTG TGG-3’
61	G443NNK_rev	5’-CCA CAA AMN NTT CAG GTT TTA ACG-3’
62	V445NNK_for	5’-CCT GAA GGC TTT NNK GTA AAA GCA -3’
63	V445NNK_rev	5’-TGC TTT TAC MNN AAA GCC TTC AGG-3’
64	T480NNK_for	5’-CGC TCA TAA TNN K CCG CTG CTT GTG-3’
65	T480NNK_rev	5’-CAC AAG CAG CGG MNN ATT ATG AGC G-3’
66	T515NNK_for	5’-CCG CAG GTC GCA NNK CTT GAT TCA C-3’
67	T515NNK_rev	5’-GTG AAT CAA GMN NTG CGA CCT GCG G-3’
68	P654NNK_for	5’-GCG GAT ATG NNK CTT GCG AAA ATG-3’
69	P654NNK_rev	5’-CAT TTT CGC AAG MNN CAT ATC CGC-3’
70	T664NNK_for	5’-GGT GCG TTT TCA NNK AAC GTC GTA GCA-3’
71	T664NNK_rev	5’-TGC TAC GAC GTT MNN TGA AAA CGC ACC-3’
72	D698NNK_for	5’-CAA GAA GGA NNK CAT TTA GGT G-3’
73	D698NNK_rev	5’-CAC CTA AAT GMN NTC CTT CTT G-3’
74	E1037NNK_for	5’-CAG CAG CTA GAA NNK AAA GGC CG -3’
75	E1037NNK_rev	5’-CGG CCT TTM NNT TCT AGC TGC TG-3’
76	BMfor_1504	5’-GCA GAT ATT GCA ATG AGC AAA GG-3’

77	BMrev1504	5’-CCT TTG CTC ATT GCA ATA TCT GC-3’
78	BMfor2315	5’-CGG TCT GCC CGC CGC ATA AAG-3’
79	BMrev2315	5’-CTT TAT GCG GCG GGC AGA CCG-3’

Enzyme library construction. HL1 library was prepared by introducing L52I, S106R, M145A, L324I, V340M, I366V, E442K substitutions into 35E11 singly and in combination by PCR overlap extension mutagenesis and SOEing. The previously described pCWori_35E11[2] served as template, BamHI_fwd and SacI_rev as megaprimers, and sequences 1 to 14 as mutagenizing primers. The amplified region (1.5 Kbp) was cloned in pCWori_35E11 using *BamH* I and *Sac* I restriction enzymes. Heme domain library HL2 was created by random mutagenesis of ETS8 heme domain residues 1-433 (*Taq* polymerase (Roche, Indianapolis, IN), BamHI_fwd and SacI_rev primers, and $MnCl_2$ from 50 to 300 μM). HL3 active-site libraries were prepared by site-saturation mutagenesis at positions 74, 75, 78, 82, 87, 88, 181, 184, 188, 260, 264, 265, 268, 328, 401, 437 and 438 using the 19A12 sequence as template. 437NNK and 437NNK sub-libraries were prepared using primers 17-20 and *BamH* I/*EcoR* I restriction enzymes (3.2 Kbp fragment). The remaining NNK libraries were created using primers 22-53 and *BamH* I/*Sac* I restriction enzymes. Heme recombination library HL4 was created by recombining mutations A74S, A74Q, V184S, V184T, V184A. HL5 heme saturation/recombination libraries were prepared by recombining mutations 74S/NNK, 82S/G, and 184S/T/NNK. RL1 and RL2 reductase domain libraries were prepared by random mutagenesis of 35E11 FMN domain (432-720) and FAD domain regions (724-1048). Error-prone PCR was carried out using *Taq* polymerase, pCWori_35E11 as template, FMN_for/FMN_rev and FAD_for/FAD_rev primer pairs, and $MnCl_2$ from 100 to 300 μM. The amplified regions were cloned in pCWori_35E11 using *Sac* I, *Nsi* I, and *EcoR* I restriction enzymes. RL3 and RL4 reductase domain libraries were created by site-saturation mutagenesis at positions 443, 445, 515, 580, 654, 664, 698, 1037 using 11-3 sequence as template, FMN_for and EcoRI_rev megaprimers, and primers 60 to 75. The amplified region (1.9 Kbp) was cloned in pCWori_11-3 using *Sac* I and *EcoR* I restriction enzymes. Library L9 was created by recombining G443A, P654K, T664G, D698G, and E1037G mutations and fusing the resulting FMN/FAD library to the 7-7 heme domain with *Sac* I and *EcoR* I restriction enzymes.

HTS and enzyme purification. High-throughput screening on dimethyl ether (DME) was carried out on 96-well plates as described.[1] Formaldehyde produced in the reaction was determined by addition of Purpald (168 mM in 2 M NaOH) and by monitoring absorbance at 550 nm. $P450_{BM3}$ variants were expressed and purified as described.[1] P450 concentration in the purified sample was measured in triplicate from the CO-binding difference spectra. Protein samples were aliquoted and stored at -80°C.

T_{50} determination. Samples of purified enzyme (~3 μM) were incubated for 10 minutes at different temperatures (from 20°C to 60°C) in a PCR thermocycler. After centrifugation, 160 μL protein solution were mixed with 40 μL 0.1 M sodium hydrosulfite on a microtiter plate. T_{50} values were calculated from heat-inactivation curves of CO-binding difference spectra (see below). Experiments were carried out in triplicate.

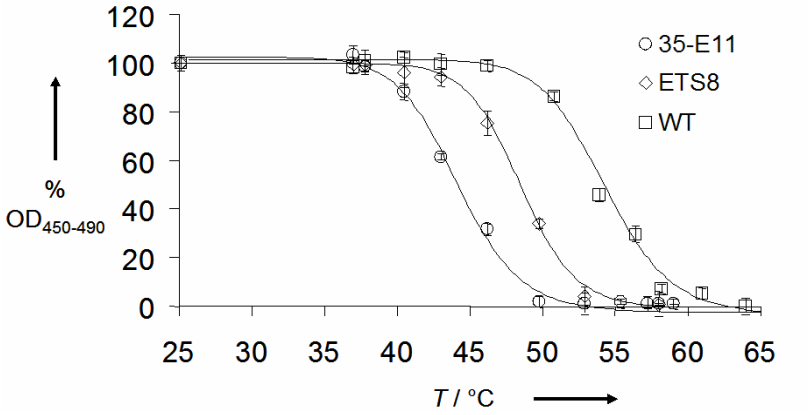

Oxidation rates, coupling efficiency, and total turnovers. Initial rates of propanol formation were determined at 25°C in 100 mM KPi pH 8.0 buffer (5 mL) using purified enzyme (100-400 nM) and propane-saturated buffer. Reactions were initiated by addition of 500 μM NADPH and stopped after 20 seconds by addition of 200 μL H_2SO_4 conc. Samples were analyzed by GC-ECD as described.[1] Initial rates of NADPH oxidation were measured by monitoring the decrease in OD_{340}. Rates were determined in triplicate and calculated over the first 20 seconds using extinction coefficient ε_{340} = 6210 M^{-1} cm^{-1}. Coupling values were calculated from the ratio of propanol formation rate to NADPH oxidation rate in the presence of propane. TTN reactions were carried out at 1 mL-scale using propane-saturated KPi buffer containing 20 nM purified protein and a cofactor regeneration system (10 U/mL isocitrate dehydrogenase, 7 mg/mL isocitrate, 0.15 mg/mL $NADP^+$). Vials were sealed and stirred for 24 hours at 4°C. Products were analyzed by GC using a Hewlett-Packard 5890 Series II Plus gas chromatograph**,** Supelco SPB-1 column (60 m x 0.52 mm x 0.5 μm film), 0.5 μL injection, FID detector, and the following separation program: 250 °C inlet, 275 °C detector, 80 °C oven for 2 min, 10°C/min gradient to 110°C, 25°C/min gradient to 275 °C, and 275 °C for 2.5 min. All measurements were performed at least in triplicate.

Whole-cell biotransformations. Biotransformations were carried out at 80 mL- and 300 mL-scale using temperature-controlled 100 mL- (Ochs-labor) and 1 L-fermenter (DasGip, 4x twin), respectively. Cells were resuspended in nitrogen-free modified M9 medium supplemented with 1% (w/v) glucose. A gas mixture of propane + air (or pure oxygen) was fed to the cells at an inlet gas flow rate of 5 and 10 L h^{-1}, respectively. In the 1 L-fermenter, pO_2 and pH were maintained at 100% and 7.2, respectively. The total amount of propanol produced in the reactions was determined summing the concentration of alcohol in the reactor and that in a bubbler connected to the reactor's gas outlet. At defined time intervals, 1 mL of cell suspension was removed, centrifuged, filtered, and subjected to GC analysis. P450 concentration in the cells was determined from CO-binding difference spectra on cell lysates obtained by sonication. Prior to bioconversions, freshly transformed cells were grown in modified M9 medium supplemented with 0.4% glucose and 1.5% yeast extract. At OD_{600} = 1.2, cells were induced with 0.25 mM IPTG and 0.25 mM δ-aminolevulininc acid and harvested after 10-12 hours. In addition to standard salts, modified M9 contained nutrients (calcium pantothenate, *p*-aminobenzoic acid, *p*-hydroxybenzoic acid, thiamine) and metals ($CoCl_2$, $CuSO_4$, $MnCl_2$, $ZnSO_4$) in trace amounts.

References

[1] M. W. Peters, P. Meinhold, A. Glieder, F. H. Arnold, *J. Am. Chem. Soc.* 2003, *125*, 13442-13450.

[2] P. Meinhold, M. W. Peters, M. M. Chen, K. Takahashi, F. H. Arnold, *ChemBiochem* 2005, *6*, 1765-1768.

[3] M. Wang, D. L. Roberts, R. Paschke, T. M. Shea, B. S. Masters, J. J. Kim, *Proc. Natl. Acad. Sci. U.S.A.* 1997, *94*, 8411-8416.

[4] A. J. Warman, O. Roitel, R. Neeli, H. M. Girvan, H. E. Seward, S. A. Murray, K. J. McLean, M. G. Joyce, H. Toogood, R. A. Holt, D. Leys, N. S. Scrutton, A. W. Munro, *Biochem. Soc. Trans.* 2005, *33*, 747-753.

[5] I. F. Sevrioukova, H. Li, H. Zhang, J. A. Peterson, T. L. Poulos, *Proc. Natl. Acad. Sci. U.S.A.* ***1999***, *96*, 1863-1868.

Table S1. Thermostabilization of 35E11. L52I, S106R, M145A, L324I, V340M, I366V, E442K mutations were introduced in variants ETS1 to ETS7. S106R and M145A mutations resulted in unfolded proteins (ETS2 and ETS7, respectively) and were not considered for further recombination.

Variant	L52I	L324I	V340M	I366V	E442K	T_{50} (°C)	ΔT_{50} (°C)
35E11						43.4 ± 0.6	**0**
ETS1	X					44.5 ± 0.3	**1.1**
ETS3		X				43.2 ± 0.1	**-0.3**
ETS4			X			46.0 ± 0.1	**2.6**
ETS5				X		47.1 ± 0.1	**3.7**
ETS6					X	45.0 ± 1.4	**1.6**
ETS8	X			X		48.5 ± 0.2	**5.1**
ETS9	X				X	46.8 ± 0.6	**3.4**
ETS10			X		X	44.2 ± 0.1	**0.8**
ETS11				X	X	46.6 ± 0.2	**3.2**
ETS12	X			X	X	misfolded	-
ETS13			X	X		misfolded	-
ETS14	X		X	X		46.1 ± 0.6	**2.7**
ETS15	X		X	X	X	47.8 ± 1.3	**4.4**
ETS16	X	X		X		45.9 ± 0.1	**2.5**
ETS17	X	X		X	X	47.2 ± 0.2	**3.8**
ETS18			X	X	X	45.5 ± 0.2	**2.1**
ETS19		X	X	X	X	45.6 ± 0.3	**2.2**
ETS20		X	X	X		44.6 ± 0.2	**1.2**
ETS21	X	X	X	X		45.8 ± 0.1	**2.4**
ETS22	X	X	X	X	X	47.0 ± 0.3	**3.6**

Figure S1. Map of the activity-enhancing reductase domain mutations on a homology model of $P450_{BM3}$ FAD-binding domain prepared on the basis of the rat cytochrome P450 reductase structure (PDB: 1AMO[3]). Structural similarity between the two is supported by a preview of the solved but not yet published structure of $P450_{BM3}$ FAD-binding domain.[4] Heme domain and FMN domain are represented as in PDB: 1BVY.[5] A 30-residue linker connects the C-terminus of the FMN-binding with the N-terminus of the FAD-binding domain (dotted line).